OPEN ACCESS
IOP Publishing
Journal of Physics D: Applied Physics
J. Phys. D: Appl. Phys. **54** (2021) 133001 (12pp)
https://doi.org/10.1088/1361-6463/abd435

## Topical Review

# Operando attenuated total reflection Fourier-transform infrared (ATR-FTIR) spectroscopy for water splitting

**A Bieberle-Hütter[1], A C Bronneberg[1], K George[1] and M C M van de Sanden[1,2]**

[1] Dutch Institute for Fundamental Energy Research (DIFFER), PO Box 6336, 5600 HH Eindhoven, The Netherlands
[2] Eindhoven University of Technology, Department of Applied Physics, PO Box 513, 5600 MB Eindhoven, The Netherlands

E-mail: a.bieberle@differ.nl

Received 24 September 2020, revised 21 November 2020
Accepted for publication 16 December 2020
Published 21 January 2021

**Abstract**

Operando attenuated total reflection Fourier-transform infrared (ATR-FTIR) spectroscopy is discussed in this paper for water splitting application. The first part of the paper focuses on the discussion of the opportunities and challenges of this method for the characterization of the solid-liquid interface in water splitting. The second part of the paper focuses on recent results and future perspectives. We present stable and robust operando ATR-FTIR measurements using low temperature processing of hematite and a set-up where the functional thin film is integrated on the ATR crystal. We find increased absorbance as a function of applied potential at wavenumber values of 1000 $cm^{-1}$–900 $cm^{-1}$ and relate this to changes in the surface species during water oxidation. We argue that this approach has the potential to be developed to a routine method for the characterization of interfaces in water splitting. Such ATR-FTIR data is of crucial importance for the validation of models in microkinetic modeling. We show some recent results of microkinetic modeling of the hematite–electrolyte interface and explain how a combination of operando ATR-FTIR measurements and microkinetic modeling enables the identification of the reaction mechanism in water splitting. We discuss how this combined approach will enable designing of tailored catalysts and accelerating their development in the future.

Keywords: water splitting, solid liquid interface, microkinetic modeling, reaction mechanism, hematite, infrared spectroscopy

(Some figures may appear in colour only in the online journal)

## 1. Introduction

According to well-known national and international climate accords [1, 2], $CO_2$ emissions have to be reduced, alternative energy sources need to be developed, and industry has to become circular. Hence, new, alternative, and sustainable energy solutions are required. Electrochemical applications are promising, since they allow storing energy in chemical bonds and are therefore the key for sustainable, synthetic

Original content from this work may be used under the terms of the Creative Commons Attribution 4.0 licence. Any further distribution of this work must maintain attribution to the author(s) and the title of the work, journal citation and DOI.

energy carriers. Among electrochemical applications, photoelectrochemical (PEC) water splitting is of particular interest, since it converts solar energy directly into a fuel that can be stored [3].

PEC is known to suffer from low efficiency and degradation of the performance. The main reason for this is that the limiting processes at the electrochemical interface—the heart of a PEC device—are not identified so far because of the complexity of the PEC interface and a lack of methodology [4–6]. Both these shortcomings are related to the fact that the PEC interface is a solid–liquid interface with many species and reactions taking place during operation. It is difficult to characterize solid–liquid interfaces during operation, since typical surface characterization tools, such as x-ray based methods or microscopy, work usually under low pressure or even at vacuum. Hence, these methods are optimized to characterize the solid–gas interface. They are usually not used to characterize the solid–liquid interface which is at atmospheric pressure and consists of a liquid phase. In addition, direct measurement methods which can measure the species during operation and allow to conclude about the reaction mechanism taking place at the interface are sparse. Therefore, the research usually relies on indirect measurement methods where physical quantities, such as the current in current–voltage measurements or the impedance in electrochemical impedance spectroscopy (EIS), are measured and the data is related and interpreted with a chemical or electrochemical model. Series of measurements are typically carried out in order to extract mechanistic information and to confirm assumed models. Such analyses lack the direct relation between the measured physical quantities (e.g. current, voltage) and the chemical quantities (e.g. rate constants, surface species) that characterize the reaction mechanism.

In addition, the species and intermediates to be measured in order to identify the reaction mechanism are often components of hydrogen and oxygen. This is not only the case in PEC, but similarly in electrolyzer or fuel cell experiments. Such species are in general difficult to measure. In addition, a variety of atomic combinations are possible and all have rather similar molecular weight so that differentiation between the species is difficult. Furthermore, the species often exist for very short times or are of intermediate nature. Therefore, very short timescales are required for measurements to identify species and intermediates.

In the literature, several paths have been followed in recent years in order to identify the reaction mechanism at PEC interfaces under operation. Most techniques rely on spectroscopy. A recent overview about experimental techniques is given by Yang *et al* [5]. A noteworthy technique is operando- x-ray photoelectron spectroscopy (XPS) [7–11]. 'Operando' (from Latin, meaning 'by operating') denotes that measurements are carried out while the cell to be investigated is set to different operating points. In operando XPS, a PEC cell is set to a certain potential and pulled out of the electrolyte while applying a potential. The surface is characterized by XPS, while still a thin layer of electrolyte is sticking on the electrode and potential is applied. This method allows for identifying the nature and the oxidation states of the surface atoms. It is not guaranteed whether the potential is frozen in by this method and whether the ultra-thin film is stable during the entire measurement.

Another frequently used technique in the field is transient absorption spectroscopy which studies the charge carrier dynamics by a pump-probe method. Various detectors can measure different time scales so that the processes taking place at the interface can be identified. In [12], it was found for example that the processes of electron extraction and electron–hole recombination at a hematite–electrolyte interface are completed within roughly 20 ms, while water oxidation is observed to occur on a timescale of hundreds of milliseconds to seconds. Since the timescale of water oxidation was found to be independent of the concentration of photogenerated holes, it was concluded that the mechanism of water oxidation on hematite takes place via a sequence of single-hole oxidation steps [12]. In contrast to this study, Mesa *et al* [13] suggested recently a reaction mechanism that is third order in surface-hole density for hematite. They used a light induced spectro-electrochemical setup that simultaneously measures the photo-induced absorption and the transient photocurrent. The proposed mechanism involves equilibration between three surface holes and M(OH)–O–M(OH) sites.

Another promising method to measure chemical species is vibrational spectroscopy. A good review on operando vibrational spectroscopy dedicated to $CO_2$ conversion is given by Heidary *et al* [14]. Main methods using vibrational spectroscopy are Raman and Fourier-transform infrared (FTIR) spectroscopy. For surface analysis, attenuated total reflection (ATR) FTIR spectroscopy, usually named ATR-FTIR spectroscopy, is most common and allows for measuring of surface species [15]. Since IR radiation is strongly absorbed by water, the confinement of the measurement to the vicinity of the surface in ATR-FTIR spectroscopy is of particular interest because the signal strength of the bulk liquid phase is reduced in relation to the signal strength of the surface species and intermediates; therefore, the solid–liquid interface can be characterized. ATR-FTIR measurements were carried out at the interface of an aqueous solution and different metal oxide surfaces, such as $TiO_2$ [14, 16, 17], $Co_3O_4$ [18] and $IrO_2$ [19]. Metal oxo, oxyl, hydroxo, peroxo, and superoxo species and intermediates have been identified and their role in the catalytic cycles has been established for different systems. It was found that the intermediates bond to different catalytic sites.

Such *in situ* ATR-FTIR measurements give a good overview about the surface species under steady state condition. However, surface species might change and intermediate species might develop during operation. A well-accepted reaction mechanism for oxygen evolution reaction (OER) at metal oxide photoanodes from Rossmeisl *et al* [20] reports for example the formation of several intermediates. The mechanism is believed to exist of four deprotonation steps with OH, O, and OOH as intermediate species. This mechanism has so far not been experimentally confirmed. ATR-FTIR measurements under operation of a PEC would be required, i.e. operando ATR-FTIR measurements; hence, ATR-FTIR measurements are carried out while the PEC cell is set to different operating points and operated under different current–voltage

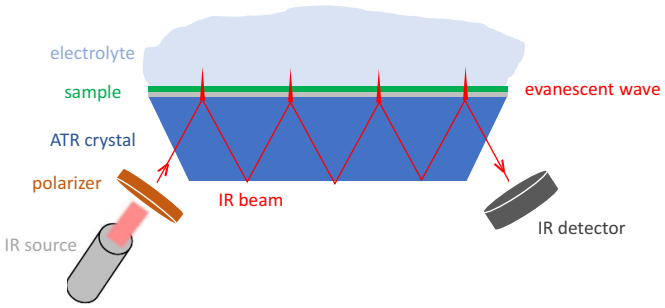


**Figure 1.** General principle of ATR-FTIR spectroscopy.

conditions. Zandi *et al* [21] and Zhang *et al* [22] carried out the first pioneering work in this direction in the field of water oxidation; Firet *et al* [23] studied the $CO_2$ electroreduction over Ag films via operando FTIR spectroscopy.

In the main part of the paper will focus on opportunities, challenges, recent results, as well as future perspectives of operando ATR-FTIR spectroscopy.

## 2. Operando ATR-FTIR for water splitting

### 2.1. Measurement principle

ATR-FTIR spectroscopy is a sampling technique based on an ATR crystal and infrared spectroscopy [24] (figure 1). A beam of infrared light is passed through an ATR crystal in such a way that the beam is reflected at the surface between crystal and adjacent medium. Different materials can be used as ATR crystals as summarized in [15]. Main properties to select a specific ATR crystal material are the wavelength cutoff and the refractive index of the crystal as well as its chemical stability in different pH range [15, 25]. If the crystal is made of an optical material with a higher refractive index than the adjacent medium, an evanescent wave is formed. The evanescent wave extends into the adjacent medium and interacts with the species at the surface and in the bulk. The light penetration depth, $d_p$, into the sample (i.e. the distance where the strength of the electric field decays to $e^{-1}$) is given by equation (1) [26, 27].

$$d_p = \frac{\lambda}{2\pi n_1 \left(\sin^2\theta - \left(\frac{n_2}{n_1}\right)^2\right)^{0.5}}, \quad (1)$$

where $\lambda$ is the wavelength of the light, $n_1$ and $n_2$ are the indices of refraction of the ATR crystal and the medium to be probed, and $\theta$ is the angle of incidence. The penetration depth is typically between 0.5 $\mu$m and 2 $\mu$m [26]. However, it should be noted that the light penetrates beyond the penetration depth and the value of $d_p$. Hence, the information that is collected from the sample can come from a depth that is 2–3 times $d_p$ [28, 29]. The number of reflections is determined by the length of the ATR crystal and the angle of incidence. The signal-to-noise ratio depends on the number of reflections as well as on the total length of the optical light path. The IR beam leaves the crystal at the opposite site of the crystal where the beam entered the crystal, and its signature is analyzed in an FTIR spectrometer. The data is in the first instance analyzed by fitting and comparing peak positions to the literature.

The ATR-FTIR method as described above is a steady state technique. It is used for a wide range of chemical (e.g. [23, 30–32]), biological (e.g. [26, 33–35]), and pharmacological (e.g. [36]) applications as well as for coatings and microfluidics (e.g. [37, 38]) in general. In the field of electrochemistry, it is important to investigate the IR signature during operation of a cell, i.e. while a potential is applied. The reason is that the species which are measured by FTIR spectroscopy, change when a potential is applied: new species, so-called intermediate species, can form. These intermediate species are formed for limited time only and they are very reactive. Measuring the intermediate species allows identifying the mechanism that takes place at the interface.

### 2.2. Measurement set-up

For operando ATR-FIT measurements, two types of set-ups are possible (figure 2). In figure 2(a), the ATR-FTIR crystal and the surface to be measured consist of two pieces; the sample surface is pressed with the active surface onto the ATR-FTIR crystal (usually a ZnSe crystal). This set-up is called in the following a 'separated set-up'. It was used in the first publications on operando ATR-FTIR studies of PEC cells by [21] and [22]. In figure 2(b), the surface to be measured is deposited on top of the ATR-FTIR crystal. The set-up is called in the following an 'integrated set-up'. Both set-ups have their advantages and disadvantages with respect to design, processing, and mounting of the sample, as well as accuracy, stability, and reproducibility of the measurement. Also, the running costs are different. In table 1, the advantages and disadvantages of both set-ups are summarized; under the section 'challenges' we discuss some of these points in more detail.

### 2.3. State-of-the-art

Only very few studies have been published on operando ATR-FTIR spectroscopy in the field of water splitting so far. In specific, two studies were published on the hematite ($Fe_2O_3$) photoanode–electrolyte system. Both studies used a separated set-up as shown in figure 2(a).

The most seminal study is from Zandi *et al* [21] where the water-oxidation reaction was studied in 0.2 M KCl (pH = 7). A potential- and light-dependent absorption peak was found at 898 $cm^{-1}$ and was assigned to a $Fe^{IV}$=O group. The assignment is based on a combined analysis of ATR-FTIR, PEC, and EIS measurements including usage of hole scavengers and isotopically labeled water, as well as comparison with density functional theory (DFT) calculations [39]. Definitive identification of the rate-determining step is not possible from these steady state measurements alone. Time resolved measurement would be required and are an exciting potential future development according to Cowan [40]. Such measurements are likely to lead to the observation of more intermediate species and to the determination of the nature of the rate-determining step.

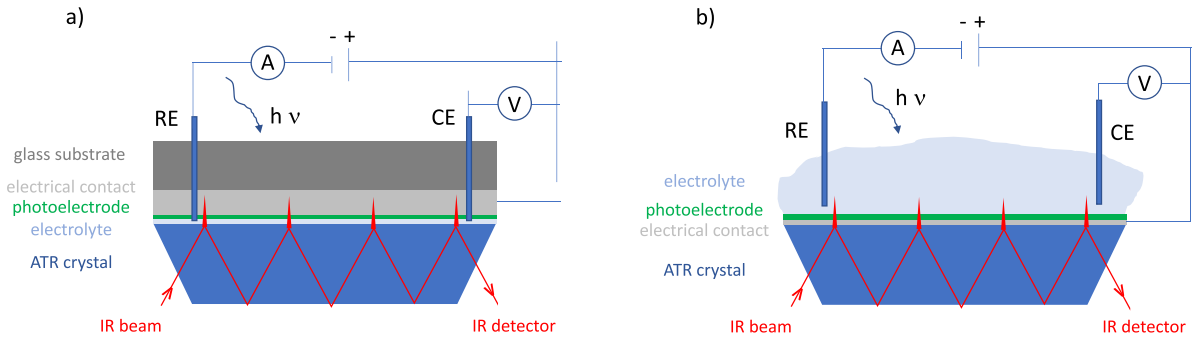


**Figure 2.** Set-ups for operando ATR-FTIR measurements: (a) separated set-up, (b) integrated set-up. The following abbreviations are used in the sketches: WE—working electrode, CE—counter electrode, RE—reference electrode, A—amperemeter, V–voltmeter.

**Table 1.** Summary of advantages and disadvantages of a separated and an integrated ATR-FTIR sample set-up.

| Criteria | | Separated set-up | Integrated set-up |
|---|---|---|---|
| Sample | Design | o | o |
| | Processing | + | − |
| | Mounting | − | + |
| Measurement | Accuracy | − | + |
| | Stability | − | + |
| | Reproducibility | − | + |
| Others | Costs | + | − |

The second important operando ATR-FTIR study on hematite was carried out by Zhang *et al* [22]. pH values between 8 and 13.6 were used and adjusted by different electrolytes consisting of 0.5 M $NaClO_4$ as well as mixtures of NaOD and $D_2SO_4$. The ATR-FTIR study was combined with the determination of the reaction order. In the near-neutral pH region, a unity rate law in combination with a surface superoxide species that was bonded via hydrogen to the adjacent hydroxyl group, was observed. Hence, a water nucleophilic attack of –Fe=O to form an O–O bond was proposed. In highly alkaline regions, the coupling of adjacent surface trapped holes on the –Fe=O species was suggested and related with a reaction order of 2.

Both studies were carried out in different electrolytes. Broad adsorption peaks were found and the spectra are rather noisy which can be related to overlapping features and/or to low sensitivity. The reproducibility as well as long term stability of the measurements were not reported. Hence, these measurements are considered as very promising first steps in identifying the reaction mechanism at hematite–electrolyte interfaces. However, more detailed investigation is required in order to fully analyze the mechanism. Main reason for the still rather preliminary data is believed to be related to complex experimental measurements (see challenges with measurement set-up below).

## 3. Opportunities

### 3.1. Identifying species and reaction mechanisms

In ATR-FTIR measurements, the wavenumber which is element and compound specific, is measured over a large range. The measured spectra can be fitted to literature data and the analysis of the peak positions allows for determining the species which are present during the measurement. Alternatively, standard compounds are measured and the sample data is compared to the standard. If by any of these methods the surface species and the intermediate species are known in a system, the reaction mechanism can be identified. Currently, already for simple interfaces, such as the hematite-electrolyte interface, the reaction mechanism taking place at the interface during operation is not unambiguously identified and different reaction mechanisms are discussed in the literature [12, 21, 22, 41]. Unambiguously identifying the species and the reaction mechanism would be a significant step in identifying the limitations at these interfaces.

### 3.2. Linking the chemistry at the interface with the electrochemical performance

Currently, the limitations at electrochemical interfaces are measured through electrochemical measurements where the performance is measured in form of current–voltage curves or EIS spectra. The current or the impedance is a measure for the performance and the limitations at the interface. However, the output data, such as the current density or the polarization resistance, is not directly related to the (electro-)chemical characteristic, i.e. the species or the rate constants. In particular, the state-of-the-art method of fitting equivalent circuit models to the EIS data results in capacitance and resistance values which are physical quantities and are not related to the chemical characteristics. Here, ATR-FTIR spectroscopy can fill the gap: By measuring the surface species and the intermediates during operation and at different operating conditions, a proven electrochemical model can be derived. This can be used as input for simulations, such as density functional theory calculations, which are carried out to determine potential determining step in water splitting, such as done for example in [20, 42]. In

this way, the chemistry at the interface and the electrochemical performance are directly linked. This allows for determining the limitations at the interface and, in consequence, for designing tailored interfaces with significantly higher performance.

### *3.3. Creating input data for microkinetic modeling and validating models*

Microkinetic modeling allows simulating electrochemical data directly from an electrochemical model, i.e. from the reactions that take place at the interface. Hence, the same data that is measured in experimental, electrochemical measurements, i.e. current–voltage curves or EIS spectra, can be simulated by microkinetic modeling. Direct comparison of experiment and simulation is possible and equivalent circuit fitting is not needed. Due to these possibilities, microkinetic modeling has recently drawn attention in the fields of water splitting [43–49] and fuel cells [50–56]. One main difficulty in microkinetic modeling is that a reaction mechanism needs to be assumed and several input parameters for the simulations are not well known, such as the surface and intermediate species or the rate constants for the reactions. Currently, the required input data are estimated from the literature or by fitting a model to experimental data. Operando ATR-FTIR spectroscopy offers an excellent opportunity to fill this gap by its ability to directly measure surface species and intermediates. The electrochemical model for the microkinetic modeling can then be derived and input parameters, such as surface species and intermediates, can be determined. If ATR-FTIR results can be quantified, even the concentrations of the species can be obtained. The most realistic input for the modeling is provided and models can be validated. After establishing the modeling for one material, the model can be transferred to other materials systems and allows for fast and inexpensive materials and parameter screening.

### *3.4. Realizing fast and flexible data collection*

Operando ATR-FTIR analyses consist of the combination of two lab-scale measurement set-ups: an ATR-FTIR spectrometer and an electrochemical measurement station. The entire set-up is rather small (lab-scale) and inexpensive. These conditions allow for a lot of flexibility. For example, systematic studies over longer times can be carried out. Different materials and processing conditions can be investigated. The surface to be analyzed can be treated between measurements in order to investigate small changes in the surface and materials properties on the formation of surface species and intermediates and the reaction mechanism. In addition, sensitive sample conditions and time sensitive measurements can be realized and carried out due to large flexibility and lab scale environment.

## 4. Challenges

### *4.1. The measurement set-up*

As shown in figure 2, two ways exist to set-up operando ATR-FTIR measurements for water splitting, i.e. the separated and the integrated way. These two ways to set-up ATR-FTIR measurements differ with respect to the mounting of the sample and the measurement compartment regarding size, electrical contacting, electrochemical configuration, and illumination. Each set-up has its own challenges; measurement reproducibility is different.

Regarding electrical contacting, it is necessary in operando ATR-FTIR measurements to realize an electrical contact on the electrode material in order to apply a bias. This electrical contact has to be spread over the entire area of the electrode, since typical electrode materials for water splitting are not sufficiently electronically conducting to guarantee a good and homogeneous current distribution with contacting at one side only. In addition, space has to be realized in the measurement compartment for the electrical contact itself. Considering a liquid electrolyte in contact with the electrode material which is often highly basic, the electrical contact needs to be isolated from the electrolyte solution. This demands for tight, nonporous materials adjacent to the electrical contacting layer.

Regarding the electrochemical configuration, one needs to be reminded that electrochemical measurements are usually carried out in three-point configuration. Hence, the set-up consists of a working electrode (WE) which is the surface to be analyzed, a counter electrode (CE) which is often a Pt wire or mesh, and the reference electrode (RE) which is in most cases a commercial Ag/AgCl glass electrode. Typical RE are rather large in diameter; typical diameters are about 1 cm. The diameters of microelectrodes are much smaller, but still in the mm range. RE are usually inserted several centimeters into the electrolyte solution. In the separated measurement set-up (figure 2(a)), however, the amount of electrolyte is limited and as few electrolyte as possible is used in order to avoid absorption of the IR beam in the electrolyte (50 $\mu$l is used for example in [21]). If the electrolyte depth is in the micrometer to millimeter range, it is obvious that placing the RE in the electrolyte and receiving good immersion of the RE at the same time is a big challenge. Small amounts of electrolyte can be well applied in the measurement compartment using calibrated pipets. However, guaranteeing a continuous and homogeneous film of electrolyte covering the sample surface is challenging. In particular for hydrophobic surfaces, un-wetted areas are difficult to be avoided. Usually, a force is used to guarantee a homogenous thin layer of electrolyte which is fully in contact with the surface to be analyzed [21]; the force needs to be applied homogenously and sample breaking has to be avoided. In addition, also with very small volume of electrolyte, it is not clear in the case of the separated set-up whether the IR signal reaches through the depth of the electrolyte to the surface of the sample considering a typical light penetration depth in the micrometer scale.

Regarding illumination, extra enclosures need to be designed in order to apply the light while guaranteeing IR radiation being confined in the set-up. In addition, the illumination has to be guaranteed to reach the foreseen intensity at the surface of the sample. This might be difficult from geometrical consideration depending on how the sample is positioned in the set-up and how much the light path might be interrupted or blocked.

These challenges indicate that the design of the measurement set-up is a crucial ingredient in guaranteeing reproducible and stable operando ATR-FTIR measurements.

### 4.2. Sample design and materials system

Several challenges arise in relation with the sample design and the materials system. In the separated measurement set-up, the same samples as in typical PEC measurements can be used. Hence, the typical sample consists of a piece of glass covered with an electrical conducting FTO (F doped $SnO_2$) layer. The photoanode material is deposited onto the FTO. In order to insert the CE and the RE electrodes, holes are usually drilled through the sample [21].

In the integrated set-up, a different sample design is required. Since the ATR crystal is very smooth (surface roughness < 2 nm), adhesion of the functional thin film is difficult to achieve. An adhesion layer is used. This adhesion layer has to be designed to be IR transparent, since the IR beam needs to transmit this layer. In addition to this adhesion layer, an electrical conducting layer has to be added for electrically contacting the electrode and in order to apply a bias. The electrical conducting layer has to have good electrical conductivity (sheet resistance < 15 $\Omega$ $cm^{-2}$), needs to be IR transparent, and well-adhering to the adhesion layer without interface reactions. The most challenging requirement for the sample design is related to the fact that the most feasible ATR crystal material for this application, i.e. ZnSe which is stable in the required pH range and has a long wavelength cutoff of about 525 $cm^{-1}$ [15], is prone to high temperature, i.e. temperatures higher than 300 °C. This requires low temperature processing of the electrical conducting layer. The typical transparent conducting oxide layer for PEC application, i.e. FTO, is therefore not an option.

Similar criteria are valid for the electrode material: low temperature processing of the electrode materials is a prerequisite as well as no interface formation or interdiffusion are allowed with the electrical conducting layer. Since in PEC often metal oxide electrodes are investigated and metal oxides are usually processed at temperatures higher than 500 °C, such requirements are not trivial to fulfill. The same morphology and materials properties of electrodes deposited on an ATR crystal substrate compared to standard FTO-glass samples are required as well.

Next to the sample design and its materials system, the electrolyte has several requirements independent of the type of measurement set-up. First, the electrolyte should not come in contact with the ATR crystal because of the danger of degradation. Note that most ATR crystals do not withstand alkaline or acidic conditions [15]. Second, the electrolyte should ideally not absorb IR radiation in the region where features form the surface species are expected in order to avoid additional IR signature from the electrolyte. This is a difficult requirement, since PEC cells are usually measured in a watery solution and water is strongly absorbing IR radiation. The usage of $D_2O$ instead of $H_2O$ is a possible solution [21, 22], since $D_2O$ is much less absorbing IR in the region where surface species are expected, i.e. between about 700 and 1000 $cm^{-1}$ [57].

### 4.3. Data acquisition and analysis

Data acquisition and analysis can be difficult when the signal-to-noise ratio of the measurement is low. Small ATR crystals have only few reflections and therefore rather low sensitivity. Increasing the size of the ATR crystal can solve this issue, however, sample preparation and contacting becomes more challenging: First, deposition of high quality metal oxide thin films over large areas (several cm range) is challenging. Second, homogeneous contact of the surface to be analyzed with the electrolyte is difficult to be realized with little volume of electrolyte in the case of the separated set-up (figure 2(a)). Third, good electrical contact and current extraction over the entire area of the surface of interest is challenging in case of insulating or semiconducting metal oxide thin films.

In addition, data analysis is hampered in case of overlapping peaks of different surface species and intermediates. All expected surface species are combinations of oxygen and hydrogen and the signatures of the different species are IR responsive in similar wavelength ranges. Hence, advanced fitting procedures and high resolution measurements with high signal-to-noise ratio are a paramount requirement. Also, the species in the electrolyte might interfere and overlap, since the IR beam is also penetrating the electrolyte even with surface sensitive ATR-FTIR measurements.

### 4.4. Stability of the samples

The stability of the entire sample has to be guaranteed under all operating conditions and over the entire measurement time. Measurement times can be rather long, since operando ATR-FTIR measurements are carried out in small intervals of applied potential and include two types of measurement, i.e. IR measurements and electrochemical characterization. Longer measurement times result in general in higher resolution. Hence, due to the number of measurements and the resolution, total measurement times of one sample of several days are possible.

It is self-evident that the surface to be analyzed has to be stable over time. However, sample stability means also that the electrolyte is not soaking into the electrode and getting in contact with the ATR crystal over time or attacking the electrical contact layer. Small pores in the layer of interest might lead to electrolyte soaking and can thus lead to instability. High quality, pore-free thin films are a prerequisite.

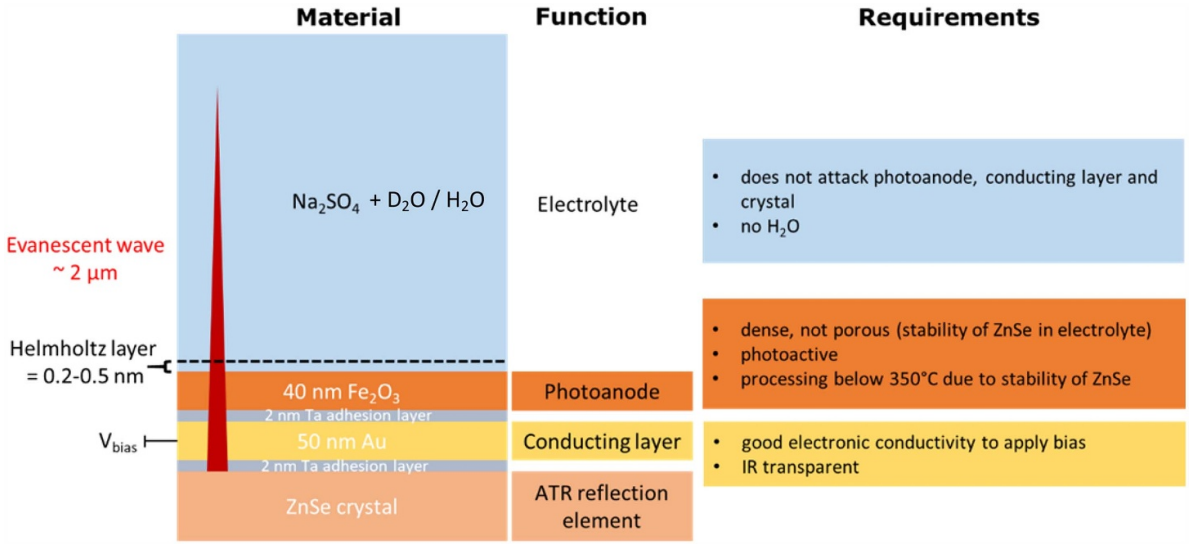


**Figure 3.** Sample design for operando ATR-FTIR measurements of water oxidation in an integrated measurement set-up as shown in figure 2(b).

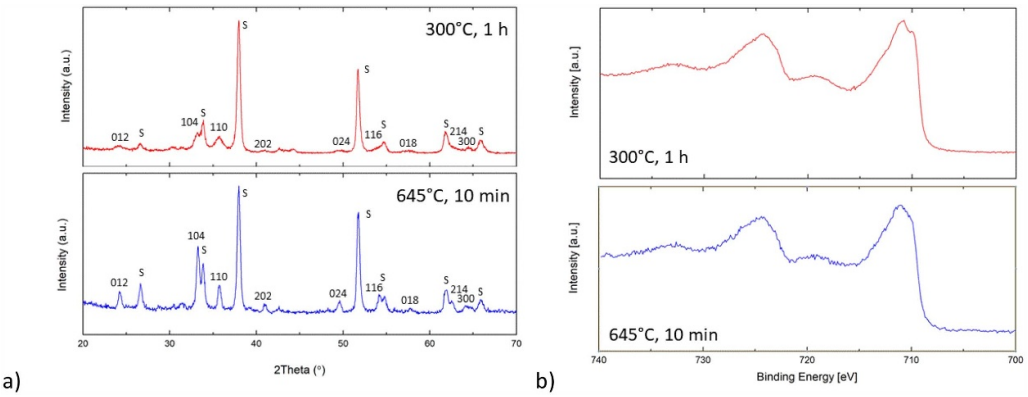


**Figure 4.** Low temperature processing of hematite thin films (300 °C, 1 h, red curves) in comparison to standard processing (645 °C, 10 min, blue curves): (a) x-ray diffraction (XRD) data (the numbers indicate the peak positions of $\alpha$-$Fe_2O_3$ according to ICDD catalogue number: 33-064; S denotes substrate peaks); (b) XPS data. The iron oxide thin films are deposited on FTO glass substrates. The data from standard processing, i.e. the blue curves, is the same as published in [58].

## 5. Recent results and future perspectives

### *5.1. Developing operando ATR-FTIR spectroscopy as a routine characterization method for water splitting*

All state-of-the-art studies in the literature were carried out in a so-called separated set-up as discussed in figure 2(a). Due to shortcomings with this type of set-up regarding to mounting of the sample, accuracy, and reproducibility of the measurement, we recently designed an alternative set-up, namely the integrated set-up (figure 2(b)). One main difference is that the surface to be analyzed is directly integrated on the ATR crystal. This set-up design has strong impact on the sample design as already mentioned in the previous chapters.

In a recent effort, we have designed a sample architecture for measuring operando ATR-FTIR data using an integrated set-up (figure 2(b)). The sample is designed as follows (figure 3): The ZnSe ATR crystal (72 mm × 10 mm × 6 mm, 45° beveled edge) was first coated with a ~2 nm thick Ta adhesion layer by sputtering. Then, a 50 nm thick Au layer was deposited on top of the Ta thin films by sputtering. The Au layer acts as IR transparent electrical contacting layer. The functional layer was made from a sputtered, 20 nm thick Fe thin film which was annealed at 300 °C for 1 h. X-ray diffraction (XRD) and XPS analyses evidenced that crystalline iron oxide thin films of hematite were obtained (figure 4). The similarity of the XRD and XPS results of low temperature annealing (red curves) and standard annealing at 645 °C for 10 min (blue curves) proves that low temperature processing of hematite thin films is a feasible route to obtain hematite. The materials selection, their function in the sample, as well as the requirements for achieving stable and high performing measurements are summarized in figure 3.

For the operando measurements, a custom-made compartment was built in-house. It was made from black Teflon in order to avoid any light reflection and it was fitted to the overhead ATR unit accessory. The ZnSe ATR crystal is

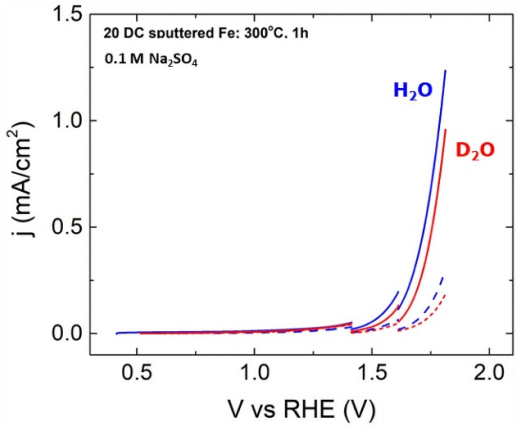


**Figure 5.** Current–voltage curves of hematite (40 nm)/Ag (50 nm)/Ta (2 nm)/ATR crystal in 0.1 M $Na_2SO_4$ in $H_2O$ (blue) and $D_2O$ (red) solution for dark (dashed line) and illuminated (continuous line) conditions, respectively. The discontinuities in the curves arise from measurements at fixed potential.

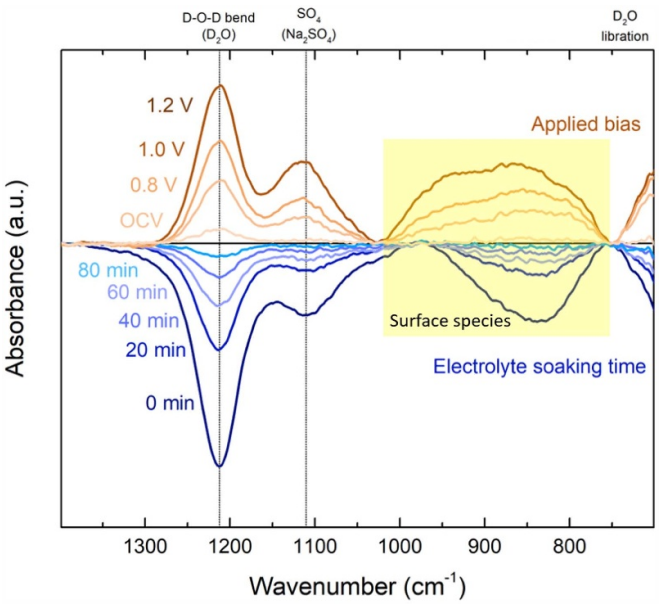


**Figure 6.** ATR-FTIR spectrum of hematite (40 nm)/Ag (50 nm)/Ta (2 nm)/ATR crystal in 0.1 M $Na_2SO_4$ with $D_2O$ under applied bias and as a function of electrolyte soaking time.

mounted from the bottom. A Kalrez O-ring ensures that the cell is leak tight and it defines the electrode area as 3.07 $cm^2$. The electrolyte reservoir has a volume of 6.45 $cm^3$. The top of the cell is open, which allows illumination of the sample and access for CE and RE. Operando electrochemical measurements were performed using a SP-150 potentiostat from Biologic using a Pt wire CE and a leak-free Ag/AgCl micro-RE (Warner Instruments). The experiments were performed in 0.1 M $Na_2SO_4$ in $H_2O$ and $D_2O$ (99.9%, Sigma Aldrich). $D_2O$ was used instead of $H_2O$ in order to avoid overlap of features in the absorption spectra from surface species and from $D_2O$ libration [43] (see 'sample design and materials system'). A 455 nm LED with an output power of ~1000 mW was used as light source. This is an ideal wavelength to stimulate oxygen evolution reaction at a hematite surface (bandgap around 2.1 eV) even with losses due to overpotential.

Figure 5 shows the current–voltage curves in $H_2O$ (blue) and $D_2O$ (red) for dark (dashed line) and illuminated (continuous line) conditions, respectively. Comparing the dark and the illuminated condition shows that the hematite layer is photoactive both in $H_2O$ as well as in $D_2O$. This is an important observation regarding the fact that the hematite thin films were annealed at a temperature of 300 °C only. The onset potential under illumination is around 1.3 V vs. RHE (reversible hydrogen electrode). The discontinuities in the curves arise from measurements at constant potential for 30 min. Only small discontinuities are found which indicates that the samples are stable over time.

The ATR-FTIR measurements were performed using a Bruker Vertex 70 FTIR spectrometer equipped with an overhead ATR unit (A537) and a liquid nitrogen cooled MCT detector. The IR spectra were recorded at 4 $cm^{-1}$ resolution in a spectral range from 3900 $cm^{-1}$ to 600 $cm^{-1}$. Steady-state spectra are averaged over 500 scans.

ATR spectra measured in the integrated set-up are shown in figure 6. On the negative $y$ axis, the ATR-FTIR spectra are plotted as a function of soaking time (0 min to 80 min; $V_{applied} = 0$ V) (blue color); on the positive $y$ direction, variations in applied potential (0 V−1.2 V vs. RHE) are plotted. All spectra are normalized to a soaking time of 100 min. Soaking time refers to the time that the sample is mounted in the compartment and the electrolyte can penetrate into the functional thin film. The data on the negative $y$ axis shows that the IR absorbance decreases as a function of soaking time over the entire wavelength range. Shortly after starting the measurement (0 min to 40 min), the difference in IR absorbance between consecutive measurements is rather strong, whereas the difference becomes small after about 60 min. We related these effects to electrolyte diffusing into the microstructure of the functional layer due to porosity. This diffusion of electrolyte into the hematite increases the amount of electrolyte that is measured and, therefore, in normalized representation to longest soaking time, the absorbance is decreasing. A good compromise between stable measurement conditions and reasonable measurement times is realized by using a soaking time of 100 min. For further studies, it is advised to fabricate functional layers with as low porosity as possible so that soaking and equilibration time can be minimized. Pores in the functional layer can be avoided by changing the thin film deposition process. Quantitative analyses of all individual contributions to the IR data is recommended then with these measurements.

In all spectra, four main features are identified: a rather narrow peak around 1200 $cm^{-1}$ which is related to D–O–D bending [59]. A peak around 1100 $cm^{-1}$ which is related to $SO_4^{2-}$ species in the electrolyte [60]. A broad peak at wavenumber values between 1000 $cm^{-1}$ and 750 $cm^{-1}$ which is attributed to adsorbed surface species [21, 22]. And finally, a feature below 750 $cm^{-1}$ which is attributed to libration of $D_2O$ [29, 61, 62].

Focusing now on the ATR-FTIR spectra as a function of applied bias (shown on the positive *y* axis), one finds an increase in absorbance with an increase in applied bias in the entire wavenumber range. We relate this overall increase in absorbance to near-surface molecules which re-orient under an applied potential and therefore result in a stronger signature [63]. In the region where surface species are expected, i.e. between 1000 $cm^{-1}$ and 750 $cm^{-1}$ (see yellow shaded area in figure 6), a broadening of the feature around 900 $cm^{-1}$–1000 $cm^{-1}$ is found. Since this feature does not change in the soaking curves (negative *y* axis), it is a clear indication that intermediates are produced as a function of applied potential. It should be noted that rather small values for the applied bias were used here and—compared to the current–voltage curve in figure 5—the applied bias of 1.2 V is just at the beginning of the onset of photocurrent. This operating condition was used, since the samples have some pores as seen in the soaking experiments and there was danger of detachment of the thin films at higher potentials.

In the literature, Zandi *et al* [21] also identified a peak around 898 $cm^{-1}$ and assigned it to R–$Fe^{IV}$=O. The features found by Zhang *et al* [22] were found around 1096 $cm^{-1}$ and attributed it to R–$Fe^{III}$–O–H–O–O–$Fe^{III}$–R. This peak is overlapping with the peak at 1100 $cm^{-1}$ in our data which was related to $SO_4^{2-}$ species according to the used electrolyte [60] (see above). From this comparison to the literature, we cannot unambiguously assign the feature around 900 $cm^{-1}$–1000 $cm^{-1}$ to a specific intermediate species. Detailed fitting is required as well as more detailed investigation of this feature as a function of potential and electrolyte composition for example. Compared to the data in [21] and [22], the spectra in figure 6 are smoother and more consistent as a function of applied potential. We attribute this to a more stable electrode configuration (RE, CE, WE) in a larger volume of electrolyte and is therefore related to the integrated measurement set-up that is used for the first time for these kind of measurements in the current study.

The above results illustrate that the integrated measurement set-up is a viable alternative to the separated set-up that is usually used in the literature for these kind of measurements. It is seen that the sample design is a critical and challenging step for realizing easy and reproducible measurements in the integrated set-up. The measured data is more stable and reproducible compared to the separated set-up. Regarding costs, it is required to establish a refurbishing process for the ATR crystals in order to re-use the crystals after one measurement.

For the future, it is important to develop an easy to use platform for operando ATR-FTIR measurements. At the moment, both measurement set-ups have advantages and disadvantages and need to be developed further in order to develop towards a standard characterization tool for identifying surface species and intermediates during operation. This would be very important for daily characterization, materials scanning, and identification of the reaction mechanism as a function of sample morphology, surface finish, and stoichiometry.

### *5.2. Identifying the reaction mechanism at electrochemical interfaces in combination with microkinetic modeling*

Operando ATR-FTIR measurements allow measuring the chemical nature of surface species and the intermediates at the same operating conditions as the electrochemical data is measured. However, as discussed before the measurements are rather challenging and the unambiguous determination of the species and their concentrations are not always possible due to overlapping peaks in the ATR-FTIR measurements. Hence, ATR-FTIR measurements are a great tool to advance in identifying the reaction mechanism at the electrochemical interface; however, complementation by other techniques might be necessary for full identification. We suggest a combination with microkinetic modeling.

As mentioned earlier, microkinetic modeling has recently evolved as an alternative method to identify the reaction mechanism at electrochemical interfaces [44–52]. In our recent microkinetic modeling studies of the hematite–electrolyte interface [44, 45], the typical model for OER from Rossmeisl *et al* [20] was assumed, i.e. a model with four consecutive deprotonation steps with the intermediate species OH, O, and OOH. This electrochemical model was implemented in a MATLAB code together with the Gerischer theory for charge transfer and the charge carrier dynamics within the semiconductor so that the electrochemical behavior at the interface was simulated [45]. Figures 7(a) and (b) show typical, simulated current–voltage curves and EIS spectra as a function of illumination and applied potential, respectively. A flat band potential of 0.6 V vs. RHE is used in the simulations here. According to figure 7(a), the current density increases strongly after the onset potential of around 1.2 V vs. RHE (figure 7(a)). The impedance decreases correspondingly (figure 7(b)), mainly based on a strong decrease of the low frequency arc. The low frequency arc is usually attributed to the intermediates at the interface [64] and the decrease of the impedance can be related to oxygen evolution reaction taking place. This effect is also seen in figure 7(c) where the coverages of the adsorbed species, OH, O, and OOH, are plotted as a function of potential together with the coverage of adsorbed $O_2$ and the total surface coverage. Around the onset potential, the amount of free surface sites decreases, while the amount of adsorbed OH is increasing around the onset potential. The coverage of OH stays high for all applied voltages after the onset potential. This indicates that the step where OH is used in the mechanism, i.e. the O formation step, is limiting here, since OH is not used up. The current density and impedance data simulated from the electrochemical model with input from atomistic calculations [42] are comparable to experimental results (refer also to similar simulations in [44, 45]).

The present intermediate species in the microkinetic modeling come straightforward from the assumed electrochemical model, i.e. the assumed reactions taking place at the interface. Currently, the reaction mechanism of Rossmeisl *et al* [20] is the most widely accepted reaction mechanism to take place at metal oxide electrodes for water splitting. However, all of

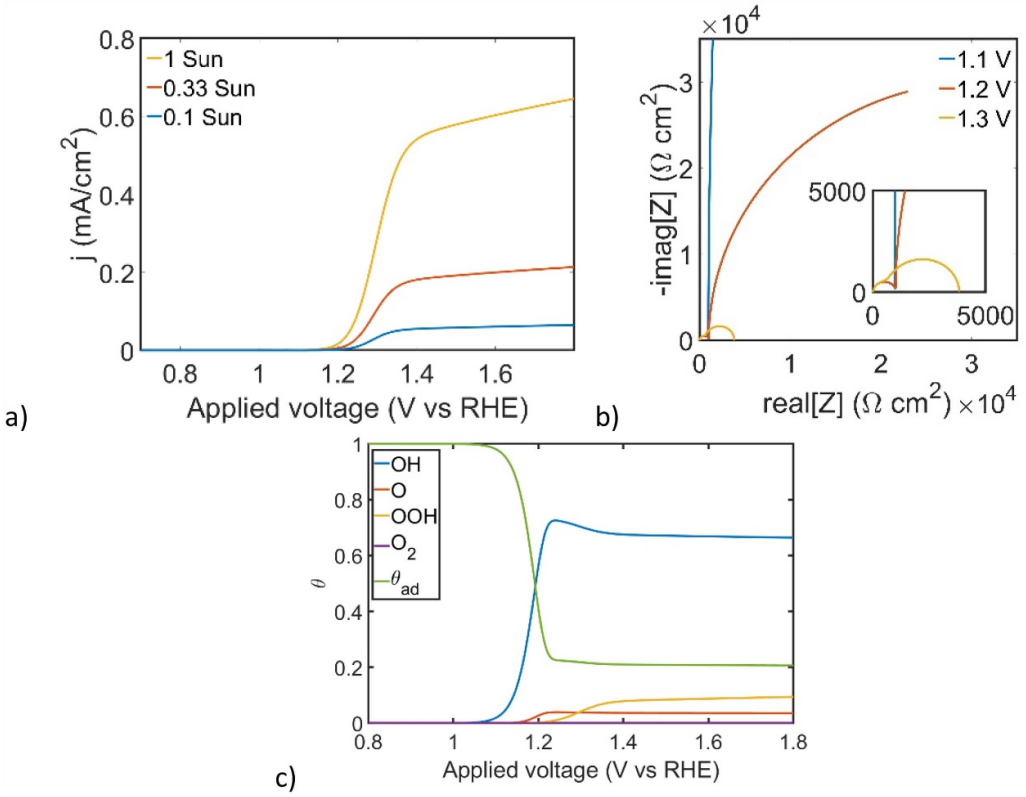


**Figure 7.** Simulated electrochemical data by microkinetic modeling: (a) current–voltage curves as a function of the illumination, (b) Nyquist EIS spectra as a function of applied potential, and (c) surface coverages of intermediate species adsorbed on the hematite surface as a function of applied potential. $\theta$ is the fractional ratio of free adsorption sites available, and $\theta_i$ is the fractional coverage of intermediate species $i$. The concentration of species $O_2$ ($\theta_{O2}$) is not visible as the coverage is small compared to the other species. Figures (b) and (c) are simulated for an illumination of 1 sun.

these intermediate species have still not been confirmed yet. Therefore, the microkinetic modeling results strongly depend on the correctness of this model. ATR-FTIR measurements can prove the surface species and intermediates and by this validate the model used in microkinetic modeling.

In contrast, ATR-FTIR measurements can mainly identify the species; it is hard to quantify this data and identify the mechanism. Here, in turn, microkinetic modeling can step in by investigating different possible mechanisms with the same intermediate species and simulate electrochemical data. If the data is comparable to experimental data, then the electrochemical model is correct.

Hence, a combination of ATR-FTIR measurements and microkinetic modeling can allow for fully identifying the reaction mechanism at the interface and for identifying the limiting process at the electrochemical interface.

### *5.3. Designing catalysts with tailored properties*

When for one system microkinetic modeling and operando ATR-FTIR spectroscopy have allowed to determine the reaction mechanism, then other materials systems can be studied as well. The same sample platform and sample processing can be used for other materials systems in the ATR-FTIR measurements. For the microkinetic modeling, the same electrochemical model and the same MATLAB code will be used in first instance. Materials specific input data, such as rate constants, will be estimated from the literature and with the help of atomistic modeling [42]. Then, the new materials system will be simulated and experiments will be carried out. A stepwise approach will finally lead to the identification of the new materials systems.

By identification of more and more materials systems and electrochemical interfaces, it might be possible to find patterns and general rules in properties and features of electrochemical interfaces and their reaction mechanisms. This will allow for designing improved catalysts with tailored properties. In addition, a significant set of data will also enable to approach the challenge of identifying the reaction mechanisms at electrochemical interfaces from the other side: since operando ATR-FTIR measurements are not yet developed to a routine and fast materials characterization tool, small changes in the materials system, for example, are related with a lot of experimental afford. Microkinetic modeling could be used here to avoid time consuming series of experiments. Microkinetic modeling codes can be developed further to enable to predict ATR-FTIR spectra. Then, only some specific experiments would be required in order to control the identification procedure. ATR-FTIR spectra could be simulated as a function of stoichiometry, morphology, defects, etc. This will allow for scanning for materials, properties, and operating conditions as well as their effects on the output data. This will save

time and costs and will accelerate the identification and design of new, high performing catalysts with tailored properties significantly.

## 6. Summary and conclusions

The great potential of operando ATR-FTIR measurements for the identification of reaction mechanisms was discussed in this paper. Operando ATR-FTIR spectroscopy allows measuring surface species and intermediates during operation, i.e. while a potential is applied and electrochemical data is recorded. Hence, information about the species involved in the electrochemical reactions at the interface can be gained and can lead to full identification of the reaction mechanism at these electrochemical interfaces.

Two types of set-ups were discussed as well as opportunities and challenges of operando ATR-FTIR measurements. We presented new results with an integrated ATR-FTIR measurement set-up which has the advantage of high quality, stability, and reproducibility of the measurement data. Based on these results, we derive several promising future perspectives: (a) development of operando ATR-FTIR spectroscopy as a routine and robust measurement method for water splitting, (b) combination of operando ATR-FTIR measurements with microkinetic modeling for model validation and identification of reaction mechanisms at electrochemical interfaces, (c) designing of tailored catalysts and accelerating catalyst development by predicting of spectroscopic data through a combination of ATR-FTIR measurements and microkinetic modeling.

In conclusion, we can state that operando ATR-FTIR measurements offer high potential to bring the field of solid–liquid electrochemical interfaces a significant step forward. In particular, this technique can enable to identify the reaction mechanism at such interfaces. This was shown with the example of PEC water splitting. However, the ATR-FTIR approach itself as well as ATR-FTIR spectroscopy in combination with microkinetic modeling, is generic and can be used for other systems as well.

## Acknowledgments

Dr A Bronneberg thanks funding in the frame of the Marie Skłodowska-Curie action of H2020 (project 'IRS-PEC' no. 708874). Dr A Bieberle-Hütter and Professor MCM van de Sanden acknowledge funding from NWO (FOM program nr. 147 '$CO_2$ neutral fuels'). In addition, Dr A Bieberle-Hütter and K George acknowledge funding from the Shell-NWO/FOM 'Computational Sciences for Energy Research' PhD program (CSER-PhD; no. i32; project no. 15CSER021) and from M-ERA.NET (project 'MuMo4PEC' no. 4089). Dr E Zoethout, DIFFER, is thanked for experimental support in materials characterization. Dr R Sinha, Dr M van Berkel, Dr Q Ong, and Dr E Langereis, DIFFER, as well as Dr R Lavrijsen, TU/e, are thanked for stimulating and fruitful discussions.

## ORCID iDs

A Bieberle-Hütter https://orcid.org/0000-0001-8794-9312
K George https://orcid.org/0000-0003-2242-8190
M C M van de Sanden https://orcid.org/0000-0002-4119-9971

## References

[1] United Nations Framework Convention on Climate Change 2020: The Paris Agreement (available at: https://unfccc.int/process-and-meetings/the-paris-agreement/the-paris-agreement)
[2] Wiebes E 2019 Dutch climate agreement (Den Hague: The Netherlands) (available at: www.klimaataccord.nl)
[3] van de Krol R and Grätzel M 2012 *Photoelectrochemical Hydrogen Production* (Berlin: Springer)
[4] Hu C, Zhang L and Gong J 2019 *Energy Environ. Sci.* **12** 2620–45
[5] Yang W, Ramanujam R, Tan J, Tilley S D and Moon J 2019 *Chem. Soc. Rev.* **48** 4979–5015
[6] Song J, Wei C, Huang Z-F, Liu C, Zen L, Wang Z and Xu Z J 2020 *Chem. Soc. Rev.* **49** 2196–214
[7] Lichterman M F *et al* 2015 *Energy Environ. Sci.* **8** 2409–16
[8] Lewerenz H *et al* 2016 *Electrochim. Acta* **211** 711–9
[9] Stoerzinger K A, Favaro M, Ross P N, Hussain Z, Liu Z, Yano J and Crumlin E J 2018 *Top. Catal.* **61** 2152–60
[10] Favaro M, Drisdell W S, Marcus M A, Gregoire J M, Crumlin E J, Haber J A and Yano J 2017 *ACS Catal.* **7** 1248–58
[11] Novotny Z *et al* 2020 *Rev. Sci. Instrum.* **91** 023103
[12] Pendlebury S R, Cowan A J, Barroso M, Sivula K, Ye J, Grätzel M, Klug D R, Tang J and Durrant J R 2012 *Energy Environ. Sci.* **5** 6304–12
[13] Mesa C A *et al* 2020 *Nat. Chem.* **12** 82–89
[14] Heidary N, Ly K H and Kornienko N 2019 *Nano Lett.* **19** 4817–26
[15] Mudunkotuwa I A, Minshid A A and Grassian V H 2014 *Analyst* **139** 870.14
[16] Nakamura R, Imanishi A, Murakoshi K and Nakato Y 2003 *J. Am. Chem. Soc.* **125** 7443–50
[17] Nakamura R and Nakato R 2004 *J. Am. Chem. Soc.* **126** 1290–8
[18] Zhang M, de Respinis M and Frei H 2014 *Nat. Chem.* **6** 362–7
[19] Sivasankar N, Weare W W and Frei H 2011 *J. Am. Chem. Soc.* **133** 12976–9
[20] Rossmeisl J, Qu Z-W, Zhu H, Kroes G-J and Norskov J K 2007 *J. Electroanal. Chem.* **607** 83–89
[21] Zandi O and Hamann T W 2016 *Nat. Chem.* **8** 778–83
[22] Zhang Y, Zhang H, Liu A, Chen C, Song W and Zhao J 2018 *J. Am. Chem. Soc.* **140** 3264–9
[23] Firet N J and Smith W A 2017 *ACS Catal.* **7** 606–12
[24] Ramer G and Lendl B 2013 *Encyclopedia of Analytical Chemistry: Attenuated Total Reflection Fourier Transform Infrared Spectroscopy* (New York: Wiley)
[25] Hind A R and Bhargava S K 2001 *Adv. Colloid Interface Sci.* **93** 91
[26] Kazarian S G and Chan K L A 2013 *Analyst* **138** 1940–51
[27] Mirabella F M Jr. 1993 *Internal Reflection Spectroscopy: Theory and Applications* (*Practical Spectroscopy Series*) (New York: Marcel Dekker) pp 17–52
[28] Mirabella F M 1983 *J. Polym. Sci. Polym. Phys. Ed.* **21** 2403–17
[29] Chan K L A and Kazarian S G 2007 *Appl. Spectrosc.* **61** 48–54
[30] Lewiner F, Klein J P, Puel F and Févotte G 2001 *Chem. Eng. Sci.* **56** 2069–84

[31] Agarwal S, Takano A, van de Sanden M C M, Maroudas D and Aydil E S 2002 *J. Chem. Phys.* **117** 10805
[32] Leewis C M, Kessels W M M, van de Sanden M C M and Niemantsverdriet J W 2006 *J. Vac. Sci. Technol.* A **24** 296
[33] Tiernan H, Byrne B and Kazarian S G 2020 *Spectrochim. Acta* A **241** 118636
[34] Naseer K, Ali A and Qazi J 2020 *Appl. Spectrosc. Rev.* (https://doi.org/10.1080/05704928.2020.1738453)
[35] Liu H and Webster T J 2007 *Biomaterials* **28** 354
[36] Pinkerneil P, Güldenhaupt J, Gerwert K and Kötting C 2012 *ChemPhysChem* **12** 2649–53
[37] Carter C F, Lange H, Ley S V, Baxendale I R, Wittkamp B, Goode J G and Gaunt N L 2010 *Org. Process Res. Dev.* **14** 393–404
[38] Chan K L A, Gulati S, Edel J B, de Mello A J and Kazarian S G 2009 *Lab Chip* **9** 2909–13
[39] Yatom N, Neufeld O and Toroker M C 2015 *J. Phys. Chem.* C **119** 24789
[40] Cowan A J 2016 *Nat. Chem.* **8** 740–1
[41] Zhang X Q and Bieberle-Hütter A 2016 *ChemSusChem* **9** 1223–42
[42] Zhang X, Klaver P, van Santen R, van de Sanden M C M and Bieberle-Hütter A 2016 *J. Phys. Chem.* C **120** 18201–8
[43] Gaiduk V I, Nielsen O F and Perova T S 2002 *J. Mol. Liq.* **95** 1–25
[44] George K, van Berkel M, Zhang X, Sinha R and Bieberle-Hütter A 2019 *J. Phys. Chem.* C **123** 9981–92
[45] George K, Khachatrjan T, van Berkel M, Sinha V and Bieberle-Hütter A 2020 *ACS Catal.* **10** 14649–60
[46] Dickens C F, Kirk C and Nørskov J K 2019 *J. Phys. Chem.* C **123** 18960–77
[47] Hansen H A, Viswanathan V and Nørskov J K 2014 *J. Phys. Chem.* C **118** 6706–18
[48] Exner K S, Sohrabnejad-Eskan I and Over H 2018 *ACS Catal.* **8** 1864–79
[49] Garcia-Osorio D A, Jaimes R, Vazquez-Arenas J, Lara R H and Alvarez-Ramirez J 2017 *J. Electrochem. Soc.* **164** E3321–28
[50] Mitterdorfer A and Gauckler L J 1999 *Solid State Ion.* **117** 203–17
[51] Mitterdorfer A and Gauckler L J 1999 *Solid State Ion.* **117** 187–202
[52] Bieberle A and Gauckler L J 2002 *Solid State Ion.* **146** 23–41
[53] Vogler M, Bieberle-Hütter A, Gauckler L, Warnatz J and Bessler W G 2009 *J. Electrochem. Soc.* **156** B663–72
[54] Bessler W G 2005 *Solid State Ion.* **176** 997–1011
[55] Rochoux M, Guo Y, Schuurman Y and Farrusseng D 2015 *Phys. Chem. Chem. Phys.* **17** 1469–81
[56] Ferreira de Morais R, Sautet P, Loffreda D and Franco A A 2011 *Electrochim. Acta* **56** 10842–56
[57] Marechal Y 2011 *J. Mol. Struct.* **1004** 146–55
[58] Sinha R, Lavrijsen R, Verheijen M A, Zoethout E, Genuit H, van de Sanden M C M and Bieberle-Hütter A 2019 *ACS Omega* **4** 9262–70
[59] Falk M 1990 *J. Raman Spectrosc.* **21** 563–7
[60] Periasamy A, Muruganaud S and Palaniswamy M 2009 *Rasayan J. Chem.* **2** 981–9
[61] Zasetsky A Y and Gaiduk V I 2007 *J. Phys. Chem.* A **111** 5599–06
[62] Silvestrelli P L, Bernasconi M and Parinello M 1997 *Chem. Phys. Lett.* **277** 478–82
[63] Bockris J O M, Reddy A K N and Gamboa-Aldeco M 2000 *Modern Electrochemistry Vol. 2A, Fundamentals of Electrodics* 2nd edn (New York: Kluwer Academic Publishers)
[64] Iandolo B and Hellman A 2014 *Angew. Chem.* **126** 13622